

DAFTAR PUSTAKA

- Anonim.(2016). Data-data lepas tentang PT International Nickle Tbk (Inco).
- Arif, I., (2018). Nikel Indonesia. PT Gramedia, Jakarta, p. 246.
- Astuti, W., Zulfiadi Z., Shofi A., Isnugroho K., Nurjaman F., dan Prasetyo E. (2012). "Pembuatan Nickel Pig Iron (NPI) dari Bijih Nikel Laterit Indonesia Menggunakan Mini Blast Furnace." Prosiding InSINas. hal. 4-6.
- Aquino, Karmina A., Arcilla, Carlo A., Schardt, Christian; Tupaz, Carmela A. J. (2022). Mineralogical and Geochemical Characterization of the Sta. Cruz Nickel Laterite Deposit, Zambales, Philippines.
- Bahfie, F. et al., (2021). Tinjauan Teknologi Proses Ekstraksi Bijih Nikel Laterit. *Jurnal Teknologi Mineral dan Batubara*, Volume 17, pp. 136-149.
- Brand, N. W., Butt, C. R. and Elias, M., (1998). Nickel laterites: Classification and Features. *AGSO Journal of Australian Geology and Geophysics*, Volume 17, pp. 81-88.
- Butt, C., (2007). "Nickel laterites characteristics, classification, and processing option". CRCLEME. *Cooperative Research Centre for Landscape Environments and Mineral Exploration*.
- Cao, Z.C., Sun, T.C., Yang, H.F., Wang, J.J., and Wu, X.D. (2010). Recovery of iron and nickel from nickel laterite ore by direct reduction roasting and magnetic separation. *Journal of University of Science and Technology Beijing* , 32(6), pp. 708-712 .
- Choiriyah. (2010). Information Gop Pengungkapan Lingkungan Hidup di Indonesia. Skripsi S1 Fakultas Ekonomi Universitas.
- Dalvi, Bacon, and Osborne. (2004). "The past and the future of nickel laterite". PDAC 2004: International convention. Trade show & investor exchange, 4(3), pp.26- 27.
- D, Ashok, Gordon Bacon, dan Robert C Osborne. (2004). The Past and the Future of Nickel Laterites. PDAC 2004 International Convention. 7 – 10 Maret 2004 Canada.
- Elliott, R., Rodrigues, F., Pickles, C. A. dan Peacey, J. (2015) "A two-stage thermal upgrading process for nickeliferous limonitic laterite ores," Canadian Metallurgical Quarterly, 54(4), hal. 395-405.
- Farrokhpay, S., Filippov, L., & Fornasiero, D. (2019). Pre-concentration of nickel in laterite ores using physical separation methods. Minerals Engineering, 141(July), 105892.

- Firdiyono, F., Ginting, I., dan Mitsutomi, K. (1983). "Pengamatan Mineralogi Laterit Nikel Pomalaa". *Metalurgi*, 3, 3-9.
- Gleeson, S., Butt, C. & El, M., (2003). Nickel Laterites : A Review. Society of Economic Geologists (SEG), July, pp. 12-18.
- Golightly, J.P. (1981)."Nickeliferous laterite deposits", *Economic Geology*(75).pp.710- 735.
- Hamada M., Ganscow S., Klimm D., Seorghio G., Reichman. J. H, and Bickermann. (2022). Wustite ($Fe_{1-x}O$) Thermodynamic and crystal growth. *Journal Zeitschrift für Naturforschung B*.
- Heslop, R. dan D.L. Robinson. (1960). Inorganic Chemistry. Elsevier Publishing Company.
- Huang, J. Hu, H. Y, F. Yang, W. Sun, (2010). Study on the technology and mechanism of magnetic roasting and separation of a refractory red iron ore, *Min. Metall. Eng.* 30. 38–41.
- Ishii, Kotaro dan Shibata. (1975). Method For Producing High-Grade FerroNickel Directly From Nickeliferous Oxide Ores. US Patent 3996045.
- Jiang, M., Sun, T., Liu, Z., Kou, J., Liu, N. dan Zhang, S. (2013) "Mechanism of sodium sulfate in promoting selective reduction of nickel laterite ore during reduction roasting process," *International Journal of Mineral Processing*, 123, hal. 32–38.
- Klacanska. M. (2017). Kalsinasi Nikel MUD. Fakultas Bahan Ilmu Dan Teknologi Di Trnava. Slovakia University Of Technology In Bratislava.
- Kuck, P.H, (2013). Nickel, U.S. Geological Survey, Mineral Commodity Summaries," <http://minerals.usgs.gov/>, 2013.
- Kyle, J., (2010), Nickel laterite processing technologies—where to next, Paper presented at the ALTA 2010 Nickel/Cobalt/Copper Conference, 24-27 May, Perth, Australia.
- Kyle, J., (2010). *Nickel Laterite Processing Technologies- Where to Next?*. Perth, ALTA 2010 Nickel/Cobalt/Copper Conference.
- Lee, H. Y., Kim, S. G. & Oh, J. K., (2005). Electrochemical leaching of nickel from low-grade laterites. *Hydrometallurgy*, Volume 77, pp. 263-268.
- Li, G., Tangming, S., Mingjun, R., Tao, J. dan Yuanbo, Z. (2012) "Beneficiation of nickeliferous laterite by reduction roasting in the presence of sodium sulfate," *Minerals Engineering*, 32, hal. 19–26.

- Lv, X., Bai, C., He, S. dan Huang, Q. (2010) "Mineral change of Philippine and Indonesia nickel lateritic ore during sintering and mineralogy of their sinter," *ISIJ International*, 50(3), hal. 380– 385.
- Ma, X., Cui, Z. dan Zhao, B. (2016) "Efficient utilization of nickel laterite to produce master alloy," *JOM*, 68(12), hal. 3006–3014.
- McDonald, R.G. and Whittington, B.I., (2008)a, Atmospheric acid leaching of nickel laterites review: Part I. Sulphuric acid technologies. *Hydrometallurgy*, 91(1–4): p. 35-55.
- Mcrae, M., E., (2019). Nickel statistics and information, U.S. Geological Survey, MineralCommoditySummaries:USA,http://www.usgs.gov/centers/nmic/nickelstatistics-and-information. Diakses pada tanggal 19 juli 2023.
- Munasir. (2012). Uji XRD dan XRF pada Bahan Mineral (Batuan dan Pasir) Sebagai Sumber Material Cerdas (CaCO_3 dan SiO_2). *Jurnal Penelitian Fisika dan Aplikasinya (JPFA)* v2n1, 20-29.
- Moskalyk, R.R., Alfantazi, A.M. (2002). Nickel laterite processing and electrowinning practice. *Miner. Eng.*, Vol. 20 (15), pp. 593–595.
- Nurjaman, F., Astuti, W., Bahfie, F., & Suharno, B. (2021). Study of selective reduction in lateritic nickel ore: Saprolite versus limonite. *Materials Today: Proceedings*, 44, 1488–1494. Norgate, T. & Jahanshahi, S., (2011). Assessing the energy and greenhouse gas footprints of nickel laterite processing. *Mineral Engineering*.
- Oxley, A. & Barcza, N., (2013). Hydro-pyro integration in the processing of nickel laterites. *International Journal of Minerals Engineering*, pp. 2-13.
- Pickles C.A., Forster J., and Elliot R. (2014). "Thermodynamic analysis of the carbothermic reduction roasting of nickeliferous limonitic laterite ore," *Minerals Engineering*., vol.65, pp. 33-40, 2014.
- Pournaderi, S., Keskkılıç, E., Geveci, A. and Topkaya, Y. A. (2014) "Reducibility of nickeliferous limonitic laterite ore from Central Anatolia," *Canadian Metallurgical Quarterly*, 53(1), pp. 26–37.
- Prasetyo, A., dan Puguh. (2011). Peningkatan Kadar Nikel dan Besi dari Bijih Nikel Laterit Kadar Rendah Jenis Saprolit untuk Bahan Baku NPI. *Jurnal Metalurgi*. Vol. 26. No. 3. Pp: 123-130.
- Prasetyo, P.; & Ronald, N. (2014). Masih Terbukanya Peluang Penelitian Proses Caron Untuk Mengolah Nikel Laterit Kadar Rendah di Indonesia. *Majalah Metalurgi*, 26, 35-44.
- Raivel, dan Firman. (2020). Karakteristik Endapan Nikel Laterit di Bawah Molasa, Daerah Tinanggea, Sulawesi Tenggara. *Jurnal GeoMining*. Program Studi Teknik Pertambangan, Fakultas Teknik. Kendari.

- Rao, M., Li, G., Zhang, X., Luo, J., Peng, Z., and Jiang, T.,(2016). “Reductive Roasting of Nickel Laterite Ore with Sodium Sulphate for Fe-Ni Production”, Part I: Reduction/Sulfidation Characteristics. *Separation Science and Technology*, (51).pp. 1408-1420.
- Rusmini, (2010). Analisis besi dalam mineral melalui proses kopresipitasi menggunakan nikel dibutil ditiokarba ma. Semarang: UNNES.
- Rodrigues, F. M., (2013), *Investigation Into The Thermal Upgrading Of Nickeliferous Laterite Ores. A thesis submitted to the Robertbuchan Departement of Mining In Corminity with the requirements for The degree of Master of applied Sciece*, Queens University, Kingston, Toronto, Canada.
- Ropp, R. C. (2013) Group 14 (C, Si, Ge, Sn, and Pb) Alkaline Earth Compunds. *Encyclopedia of the Alkaline Earth Compounds*, 351 – 480.
- Santoso, B. dan Subagio, (2018). Pemodelan Nikel Laterit Berdasarkan Data Resistivitas Di Daerah Kabaena Selatan Kabupaten Bombana, Provinsi Sulawesi Tenggara The Laterite Nickel Modelling Based On Resistivity Data, In South Kabaena, Bombana District, Southeast Sulawesi Province. *Jurnal Geologi dan Sumberdaya Mineral*, Departemen Geokimia, Universitas Padjajaran, jalan Diponegoro, Bandung.
- Sembiring. M dan Sinaga, T. (2003). Arang Aktif (Pengenalan Dan Proses Pembuatannya). Medan: Universitas Sumatra Utara.
- Sembiring, S., & Simanjuntak, W. (2015). Silika Sekam Padi Potensinya Sebagai Bahan Baku Keramik Industri (Vol. 148). Plantaxia.
- Setiawan, I., (2016). Pengolahan Nikel Laterit Secara Pirometalurgi: Kini Dan Penelitian Kedepan. Seminar Nasional Sains dan Teknologi. Pp 1-7
- Sufriadin, (2013), Mineralogi, Geokimia dan Sifat Leaching pada Endapan Laterit Nikel Sorowako, Sulawesi Selatan Indonesia, Universitas Gadjahmada.
- Tarumingkeng Stephanie. (2016). Termodinamika Dalam Memahami Proses Pengolahan Mineral Prodi Fisika FMIPA Institut Teknologi Bandung.
- Warner, A. E. M., Díaz, C. M., Dalvi, A. D., Mackey, P. J., Tarasov, A. V., & Jones, R. T. (2007). JOM world nonferrous smelter survey Part IV: Nickel: Sulfide. *Jom*, 59(4), 58–72.
- Wills, B. A., and Napiermunn, T., (2006). *Mineral Processing Technology: An Introduction to the Practical Aspects of Ore Treatment and Mineral Recovery*, 7th ed. Elsevier. Burlington.
- Y. Qu, L. Xing, L. Shao, Y. Luo, Z. Zou, (2019). Microstructural characterization and gas-solid reduction kinetics of iron ore fines at high temperature, *Powder Technol.* 355. 26–36.

- Y. Lu, Z. Wei, Y. Wang, J. Zhang, G. Li, Y. Zhang, (2019). Research on the characteristics and kinetics of direct reduction of limonite ore fines under CO atmosphere in a rotary drum reactor, Powder Technol. 352. 240–250. <https://doi.org/10.1016/j.powtec.2019.04.069>.
- Zhu, D. Q., Cui, Y., Vining, K., Hapugoda, S., Douglas, J., Pan, J. dan Zheng, G. L. (2012) “Upgrading low nickel content laterite ores using selective reduction followed by magnetic separation,” *International Journal of Mineral Processing*, 106–109, hal. 1–7.

LAMPIRAN

LAMPIRAN 1**HASIL ANALISIS X-RAY DIFFRACTION (XRD)**

1. Sampel Awal

Match! Phase Analysis Report

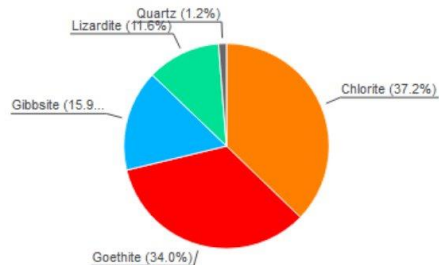
Sample: Shinta-SampelAwal

Sample Data

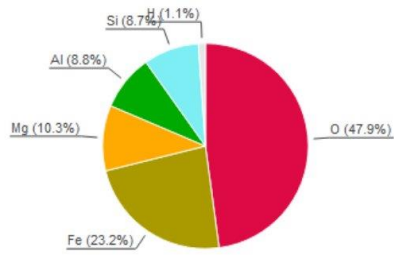
File name	Shinta-SampelAwal.txt
File path	E:/BISMILLAH TA SHINTA/SKRIPSI/Shinta-SampelAwal
Data collected	Sep 29, 2023 11:57:32
Data range	5.000° - 70.000°
Original data range	5.000° - 70.000°
Number of points	3251
Step size	0.020
Rietveld refinement converged	No
Alpha2 subtracted	No
Background subtr.	No
Data smoothed	Yes
Radiation	X-rays
Wavelength	1.541874 Å

Analysis Results

Phase composition (Weight %)



Elemental composition (Weight %)



IndexAmountName

	(%)	Name
A	37.2	Chlorite
B	34.0	Goethite
C	15.9	Gibbsite
D	11.6	Lizardite
E	1.2	Quartz
	1.3	Unidentified peak area

Formula sum

A10.865 Fe0.255 H4 Mg2.292 O9 Si1.588
 Fe H O2
 Al O3

Element Amount (weight %)

O	47.9% (*)
Fe	23.2%
Mg	10.3%
Al	8.8%
Si	8.7%
H	1.1% (*)
*LE (sum)	49.0%

Amounts calculated by RIR (Reference Intensity Ratio) method

Details of identified phases

A: Chlorite (37.2 %)*

Formula sum: A10.865 Fe0.255 H4 Mg2.292 O9 Si1.588

Entry number: 96-901-0164

Figure-of-Merit (FoM): 0.576327*

Total number of peaks: 600

Peaks in range: 312

Peaks matched: 98

Intensity scale factor: 0.21*

Space group: C 1 2/m 1

Crystal system: monoclinic

Unit cell: $a = 5.3363 \text{ \AA}$ $b = 9.2400 \text{ \AA}$ $c = 14.3700 \text{ \AA}$ $\beta = 96.930^\circ$

I/I_c: 0.69

Calc. density: 2.700 g/cm³

Reference: Zanazzi P. F., Montagnoli M., Nazzareni S., Comodi P., "Structural effects of pressure on monoclinic chlorite: a single-crystal study", American Mineralogist **92**, 655-661 (2007)

B: Goethite (34.0 %)*

Formula sum	Fe H O ₂
Entry number	96-900-2160
Figure-of-Merit (FoM)	0.749632*
Total number of peaks	364
Peaks in range	74
Peaks matched	45
Intensity scale factor	0.65*
Space group	P n m a
Crystal system	orthorhombic
Unit cell	a= 9.9189 Å b= 3.0148 Å c= 4.5835 Å
I/c	2.38
Calc. density	4.306 g/cm ³
Reference	Gualtieri A., Venturelli P., "In situ study of the goethite-hematite phase transformation by real timesynchrotron powder diffractionSample at T = 156 C", American Mineralogist 84 , 895-904 (1999)

C: Gibbsite (15.9 %)

Formula sum	Al O ₃
Entry number	96-901-5977
Figure-of-Merit (FoM)	0.000000
Total number of peaks	996
Peaks in range	348
Peaks matched	119
Intensity scale factor	0.23
Space group	P 1 21/n 1
Crystal system	monoclinic
Unit cell	a= 8.6410 Å b= 5.0700 Å c= 9.7200 Å β= 85.430 °
I/c	1.79
Calc. density	2.347 g/cm ³
Reference	Megaw H., "The crystal structure of Hydargillite Al (O H) ₃ _cod_database_code 1011081", Zeitschrift fur Kristallographie 87 , 185-204 (1934)

D: Lizardite (11.6 %)*

Formula sum	H ₄ Mg ₃ O ₉ Si ₂
Entry number	96-900-0849
Figure-of-Merit (FoM)	0.467227*
Total number of peaks	224
Peaks in range	56
Peaks matched	18
Intensity scale factor	0.13*
Space group	P 3 1 m
Crystal system	trigonal (hexagonal axes)
Unit cell	a= 5.3320 Å c= 7.2330 Å
I/c	1.35
Calc. density	2.584 g/cm ³
Reference	Mellini M., "The crystal structure of lizardite 1T: hydrogen bonds and polytypism", American Mineralogist 67 , 587-598 (1982)

E: Quartz (1.2 %)

Formula sum	O ₂ Si
Entry number	96-900-0776
Figure-of-Merit (FoM)	0.000000
Total number of peaks	140
Peaks in range	36
Peaks matched	11
Intensity scale factor	0.03
Space group	P 32 2 1 S
Crystal system	trigonal (hexagonal axes)
Unit cell	a= 4.9160 Å c= 5.4054 Å
I/c	2.95
Calc. density	2.646 g/cm ³
Reference	Levien L., Prewitt C. T., Weidner D. J., "Structure and elastic properties of quartz at pressureP = 1 atm", American Mineralogist 65 , 920-930 (1980)

(*2theta values have been shifted internally for the calculation of the amounts, the intensity scaling factors as well as the figure-of-merit (FoM), due to the active search-match option 'Automatic zero point adaption'.

Candidates

Name	Formula	Entry No.	FoM
Neon	Ne	96-901-1723	0.6112
Li _{0.77} (Ni _{0.7} Fe _{0.15} Co _{0.15}) _{1.03} O ₂	Nb Zr	96-153-7846	0.5676
Li Co _{0.333} Ni _{0.333} Mn _{0.333} O ₂	Co _{0.1545} Fe _{0.1545} Li _{0.77} Ni _{0.721} O ₂	96-152-6305	0.5476
(Li _{0.99} Ni _{0.01}) (Ni _{0.70} Co _{0.15} Al _{0.15}) O ₂	Co _{0.333} Li Mn _{0.333} Ni _{0.333} O ₂	96-400-2444	0.5456
Lithium Cobalt Oxide	Al _{0.15} Co _{0.15} Li _{0.99} Ni _{0.71} O ₂	96-153-3586	0.5448
(Li _{0.82} Ni _{0.026}) Ni _{0.994} O ₂	Co Li _{1.43} O ₂	96-155-0400	0.5388
Li (Cr _{0.167} Li _{0.277} Mn _{0.556}) O ₂	Li _{0.82} Ni _{1.02} O ₂	96-152-6281	0.5373
Li (Cr _{0.25} Li _{0.25} Mn _{0.5}) O ₂	Cr _{0.167} Li _{1.277} Mn _{0.556} O ₂	96-153-2835	0.5251
(Li _{0.88} Mg _{0.02}) (Ni _{0.92} Mg _{0.08}) O ₂	Cr _{0.25} Li _{1.25} Mn _{0.5} O ₂	96-153-2836	0.5250
(Li _{0.98} Ni _{0.02}) (Li _{0.05} Ni _{0.75} Co _{0.1} Mn _{0.1}) O ₂	Li _{0.88} Mg _{0.1} Ni _{0.92} O ₂	96-152-6285	0.5075
	Co _{0.1} Li _{1.03} Mn _{0.1} Ni _{0.77} O ₂	96-152-0790	0.5026
	Li _{0.65} Ni _{1.08} O ₂	96-153-5513	0.5013

Spinel	Al2.401 Mg0.398 O4	96-900-5769	0.4197
Spinel	Al2 Mg O4	96-900-5768	0.4173
Spinel	Al1.88 Fe0.225 Mg0.887 Mn0.005 Ni2 O4 Zn0.00196-900-5346	0.3825	
Spinel (Li, Ti)	Li0.03 O4 Ti2	96-100-8792	0.0000
Spinel (Li, Ti)	Li0.89 O4 Ti2	96-100-8793	0.0000
Spinel (Li, Ti)	Li0.75 O4 Ti2	96-100-8794	0.0000
Iron diiron(III) oxide (Magnetite)	Fe3 O4	96-101-1033	0.0000
Aluminium hydroxide (Gibbsite)	Al H3 O3	96-101-1082	0.0000
Iron diiron(II) oxide (Magnetite)	Fe3 O4	96-101-1085	0.0000
Silicon oxide \$-alpha (Quartz low)	O2 Si	96-101-1098	0.0000
Trimagnesium dihydroxide phyllo-tetrasilicate (Talc 2M)	H2 Mg3 O12 Si4	96-101-1153	0.0000
Silicon oxide (Quartz low)	O2 Si	96-101-1160	0.0000
Silicon oxide \$-alpha (Quartz low)	O2 Si	96-101-1173	0.0000
Silicon oxide - \$-alpha (Quartz low)	O2 Si	96-101-1177	0.0000
Silicon oxide - 1b (Quartz high)	O2 Si	96-101-1201	0.0000
Silicon oxide (Quartz high)	O2 Si	96-110-0020	0.0000
Montmorillonite	Al2 Ca O12 Si4	96-110-1055	0.0000
Aluminium hydroxide (Gibbsite)	Al H3 O3	96-120-0017	0.0000
Lithium Manganese Oxide (0.78/1.88/4) (Unnamed_Spinel)	Li0.78 Mn1.88 O4	96-151-4008	0.0000
Lithium Manganese Oxide (1/2/4) (Unnamed_Spinel)	Li Mn2 O4	96-151-4042	0.0000
Lithium Manganese Oxide (1/2/4) (Unnamed_Spinel)	Li Mn2 O4	96-151-4043	0.0000
Lithium Manganese Oxide (1/2/4) (Unnamed_Spinel)	Li Mn2 O4	96-151-4051	0.0000
Magnetite	Fe3 O4	96-153-9748	0.0000
Zn2TiO4 ordered spinel	O4 Ti Zn2	96-154-4335	0.0000
LiFe5O8 ordered spinel	Fe5 Li O8	96-154-4336	0.0000
LiZnNbO4 ordered spinel	Li Nb O4 Zn	96-154-4337	0.0000
Al(OH)3 gibbsite (gibbsite)	Al H3 O3	96-154-4376	0.0000
Zn2TiO4 cubic spinel	O4 Ti Zn2	96-154-4563	0.0000
Zn1.92Ti0.84Ta0.16O4 cubic spinel	O4 Ta0.16 Ti0.84 Zn1.92	96-154-4565	0.0000
Zn1.925Ti0.85Ta0.15O4 cubic spinel	O4 Ta0.15 Ti0.85 Zn1.925	96-154-4566	0.0000
Zn1.93Ti0.86Ta0.14O4 cubic spinel	O4 Ta0.14 Ti0.86 Zn1.93	96-154-4567	0.0000
Zn1.95Ti0.9Ta0.1O4 cubic spinel	O4 Ta0.1 Ti0.9 Zn1.95	96-154-4568	0.0000
Zn1.7Ti0.4Ta0.6O4 tetragonal spinel	O4 Ta0.6 Ti0.4 Zn1.7	96-154-4569	0.0000
Zn1.925Ti0.85Ta0.15O4 tetragonal spinel	O4 Ta0.15 Ti0.85 Zn1.925	96-154-4570	0.0000
Zn1.925Ti0.85Ta0.15O4 cubic spinel	O4 Ta0.15 Ti0.85 Zn1.925	96-154-4576	0.0000
(Co0.4Al0.4)Al2O4 defect spinel	Al2.4 Co0.4 O4	96-154-5122	0.0000
Zn2SiO4 modified spinel (Zn2SiO4 wadsleyite phase)	O4 Si Zn2	96-154-9040	0.0000
Zn2GeO4 cubic spinel	Ge O4 Zn2	96-154-9041	0.0000
Zn2GeO4 tetragonal spinel	Ge O4 Zn2	96-154-9042	0.0000
spinel (Ni0.15Al0.85)(Ni0.425Al0.475Cr0.1)2O4 and 880 others...	Al1.8 Cr0.2 Ni O4	96-155-9487	0.0000

Search-Match

Settings

Reference database used	COD-Inorg 2023.06.06
Automatic zero point adaptation	Yes
Downgrade entries with low scaling factors	Yes
Minimum figure-of-merit (FoM)	0.50
2theta window for peak corr.	0.30 deg.
Minimum rel. int. for peak corr.	0
Parameter/influence 2theta	0.50
Parameter/influence intensities	0.50
Parameter/multiple/single phase(s)	0.50

Criteria for entries added by user

Reference:

Entry number: 96-101-1153;96-300-0049;96-900-8041;96-900-8298;96-900-8732;96-901-4436;96-901-7404;96-110-1055;96-900-2780;96-901-0957;96-901-0958;96-901-0959;96-901-0960;96-101-1033;96-101-1085;96-153-9748;96-722-8111;96-900-0927;96-900-0928;96-900-0929;96-900-0930;96-900-0931;96-900-0932;96-900-0933;96-900-0934;96-900-0935;96-900-2317;96-900-2318;96-900-2319;96-900-2320;96-900-2321;96-900-2322;96-900-2323;96-900-2324;96-900-2325;96-900-2326;96-900-2327;96-900-2328;96-900-2329;96-900-2330;96-900-2331;96-900-2332;96-900-2333;96-900-2674;96-900-2675;96-900-4088;96-900-4156;96-900-4157;96-900-5813;96-900-5814;96-900-5815;96-900-5816;96-900-5817;96-900-5837;96-900-5838;96-900-5839;96-900-5840;96-900-5841;96-900-5842;96-900-5843;96-900-6185;96-900-6190;96-900-6195;96-900-6200;96-900-6243;96-900-6248;96-900-6253;96-900-6266;96-900-6921;96-900-6922;96-900-6923;96-900-7645;96-900-7707;96-900-7708;96-900-9769;96-900-9770;96-901-0940;96-901-0941;96-901-0942;96-901-3530;96-901-3531;96-901-3532;96-901-3533;96-901-3534;96-901-3535;96-901-6802;96-901-6803;96-901-6804;96-901-6805;96-901-6806;96-901-6807;96-901-6808;96-901-6809;96-901-6810;96-901-6811;96-901-6812;96-901-6813;96-901-6814;96-901-6815;96-901-6816;96-901-6817;96-901-6818;96-901-7087;96-901-7088;96-900-0849;96-900-1092;96-900-1093;96-900-1639;96-900-1640;96-900-1779;96-900-1883;96-900-4509;96-900-4510;96-900-4511;96-900-4512;96-900-4513;96-900-4514;96-900-4994;96-900-4995;96-900-7425;96-901-4665;96-901-5164;96-901-5487;96-901-5581;96-901-6051;96-901-6148;96-901-7502;96-101-1098;96-101-1160;96-101-1173;96-101-1177;96-101-1201;96-110-0020;96-500-0036;96-900-0776;96-900-0777;96-900-0778;96-900-0779;96-900-0780;96-900-0781;96-900-5018;96-900-5019;96-900-5020;96-900-5021;96-900-5022;96-900-5023;96-900-5024;96-900-5025;96-900-5026;96-900-5027;96-900-5028;96-900-5029;96-900-5030;96-900-5031;96-900-5032;96-900-5033;96-900-5034;96-900-7379;96-900-8093;96-900-8094;96-900-9667;96-901-0145;96-901-0146;96-901-0147;96-901-1494;96-901-1495;96-901-1496;96-901-1497;96-901-2601;96-901-2602;96-901-2603;96-901-2604;96-901-2605;96-901-2606;96-901-3322;96-901-5023;96-101-1082;96-120-0017;96-154-4376;96-900-3875;96-900-8238;96-901-1748;96-901-5516;96-901-5977;96-100-8792;96-100-8793;96-100-8794;96-151-4008;96-151-4043;96-151-4051;96-154-

4335;96-154-4336;96-154-4337;96-154-4563;96-154-4565;96-154-4566;96-154-4567;96-154-4568;96-154-
 4569;96-154-4570;96-154-4576;96-154-5122;96-154-9040;96-154-9041;96-154-9042;96-155-9487;96-155-
 9488;96-221-0103;96-400-1006;96-500-0121;96-591-0029;96-810-3495;96-810-3496;96-810-5667;96-900-
 1365;96-900-1366;96-900-1367;96-900-1368;96-900-1369;96-900-1370;96-900-1371;96-900-1372;96-900-
 1373;96-900-1374;96-900-1375;96-900-1376;96-900-1377;96-900-1378;96-900-1422;96-900-1433;96-900-
 1434;96-900-1435;96-900-1436;96-900-1437;96-900-1438;96-900-1439;96-900-1440;96-900-1441;96-900-
 1442;96-900-1443;96-900-1444;96-900-1445;96-900-1693;96-900-1694;96-900-2045;96-900-2046;96-900-
 2047;96-900-2048;96-900-2049;96-900-2050;96-900-2051;96-900-2052;96-900-2053;96-900-2054;96-900-
 2055;96-900-2056;96-900-2057;96-900-2058;96-900-2059;96-900-2060;96-900-2061;96-900-2062;96-900-
 2063;96-900-2064;96-900-2065;96-900-2066;96-900-2067;96-900-2068;96-900-2069;96-900-2070;96-900-
 2071;96-900-2072;96-900-2073;96-900-2074;96-900-2075;96-900-2076;96-900-2077;96-900-2078;96-900-
 2079;96-900-2080;96-900-2081;96-900-2082;96-900-2083;96-900-2084;96-900-2085;96-900-2086;96-900-
 2087;96-900-2088;96-900-2089;96-900-2090;96-900-2091;96-900-2092;96-900-2093;96-900-2094;96-900-
 2095;96-900-2096;96-900-2097;96-900-2098;96-900-2099;96-900-2100;96-900-2101;96-900-2102;96-900-
 2103;96-900-2104;96-900-2105;96-900-2106;96-900-2107;96-900-2108;96-900-2109;96-900-2110;96-900-
 2111;96-900-2112;96-900-2113;96-900-2114;96-900-2115;96-900-2116;96-900-2117;96-900-2118;96-900-
 2119;96-900-2120;96-900-2121;96-900-2122;96-900-2123;96-900-2124;96-900-2125;96-900-2126;96-900-
 2127;96-900-2128;96-900-2129;96-900-2130;96-900-2131;96-900-2132;96-900-2133;96-900-2134;96-900-
 2135;96-900-2136;96-900-2137;96-900-2138;96-900-2139;96-900-2140;96-900-2164;96-900-2165;96-900-
 2166;96-900-2167;96-900-2168;96-900-2169;96-900-2393;96-900-2394;96-900-2395;96-900-2396;96-900-
 2397;96-900-2398;96-900-2399;96-900-2400;96-900-2401;96-900-2402;96-900-2403;96-900-2404;96-900-
 2405;96-900-2406;96-900-2407;96-900-2735;96-900-2736;96-900-2737;96-900-2738;96-900-2739;96-900-
 2740;96-900-2741;96-900-2742;96-900-2743;96-900-2744;96-900-2745;96-900-2746;96-900-2747;96-900-
 2748;96-900-2749;96-900-2750;96-900-2751;96-900-2752;96-900-2753;96-900-2754;96-900-2755;96-900-
 2756;96-900-2757;96-900-2758;96-900-2759;96-900-2784;96-900-2845;96-900-2846;96-900-2847;96-900-
 2848;96-900-2849;96-900-2850;96-900-2851;96-900-2852;96-900-2853;96-900-2854;96-900-2855;96-900-
 2856;96-900-2857;96-900-2858;96-900-2859;96-900-2860;96-900-2861;96-900-2862;96-900-2863;96-900-
 2864;96-900-2865;96-900-2866;96-900-3480;96-900-3481;96-900-3482;96-900-3483;96-900-3484;96-900-
 3485;96-900-3486;96-900-3487;96-900-3488;96-900-3489;96-900-3532;96-900-3533;96-900-3534;96-900-
 3535;96-900-3536;96-900-3537;96-900-3538;96-900-3539;96-900-3540;96-900-3541;96-900-3542;96-900-
 3543;96-900-3544;96-900-3545;96-900-3546;96-900-3547;96-900-3548;96-900-3895;96-900-3896;96-900-
 3897;96-900-3898;96-900-3899;96-900-3900;96-900-3901;96-900-3902;96-900-3903;96-900-3904;96-900-
 3905;96-900-3906;96-900-3907;96-900-3908;96-900-3909;96-900-3910;96-900-3911;96-900-3912;96-900-
 3913;96-900-3914;96-900-3915;96-900-3916;96-900-3917;96-900-3918;96-900-3919;96-900-3920;96-900-
 3921;96-900-3922;96-900-3923;96-900-3924;96-900-3925;96-900-3926;96-900-3927;96-900-3928;96-900-
 3929;96-900-3930;96-900-3931;96-900-3932;96-900-3933;96-900-3934;96-900-3935;96-900-3936;96-900-
 3937;96-900-3938;96-900-3939;96-900-3940;96-900-3941;96-900-3942;96-900-3943;96-900-3944;96-900-
 3945;96-900-3946;96-900-3947;96-900-3948;96-900-3949;96-900-3950;96-900-3951;96-900-3952;96-900-
 3953;96-900-3954;96-900-3955;96-900-3956;96-900-3957;96-900-3958;96-900-3959;96-900-3960;96-900-
 3961;96-900-3962;96-900-3963;96-900-3964;96-900-3965;96-900-3966;96-900-3967;96-900-3968;96-900-
 3969;96-900-3970;96-900-3971;96-900-3972;96-900-3973;96-900-3974;96-900-3975;96-900-3976;96-900-
 3977;96-900-3978;96-900-3979;96-900-3980;96-900-3981;96-900-3982;96-900-3983;96-900-3984;96-900-
 3985;96-900-4938;96-900-4941;96-900-4943;96-900-4946;96-900-4947;96-900-4948;96-900-5204;96-900-
 5205;96-900-5206;96-900-5207;96-900-5208;96-900-5209;96-900-5210;96-900-5211;96-900-5212;96-900-
 5213;96-900-5214;96-900-5215;96-900-5216;96-900-5217;96-900-5218;96-900-5219;96-900-5220;96-900-
 5223;96-900-5224;96-900-5225;96-900-5226;96-900-5227;96-900-5228;96-900-5229;96-900-5230;96-900-
 5231;96-900-5232;96-900-5233;96-900-5292;96-900-5346;96-900-5347;96-900-5348;96-900-5349;96-900-
 5350;96-900-5351;96-900-5352;96-900-5353;96-900-5354;96-900-5355;96-900-5356;96-900-5357;96-900-
 5358;96-900-5359;96-900-5360;96-900-5361;96-900-5362;96-900-5363;96-900-5364;96-900-5365;96-900-
 5366;96-900-5368;96-900-5475;96-900-5477;96-900-5478;96-900-5593;96-900-5594;96-900-5595;96-900-
 5596;96-900-5597;96-900-5598;96-900-5599;96-900-5613;96-900-5614;96-900-5615;96-900-5616;96-900-
 5617;96-900-5618;96-900-5619;96-900-5620;96-900-5621;96-900-5622;96-900-5623;96-900-5624;96-900-
 5625;96-900-5809;96-900-5810;96-900-5811;96-900-5812;96-900-6570;96-900-6571;96-900-6572;96-900-
 6573;96-900-6574;96-900-6575;96-900-6576;96-900-6577;96-900-6578;96-900-6579;96-900-6580;96-900-
 6628;96-900-6629;96-900-6630;96-900-6631;96-900-6632;96-900-6633;96-900-6634;96-900-6635;96-900-
 6636;96-900-7077;96-900-7078;96-900-7079;96-900-7080;96-900-7081;96-900-7082;96-900-7083;96-900-
 7084;96-900-7085;96-900-7086;96-900-7087;96-900-7088;96-900-7089;96-900-7090;96-900-7091;96-900-
 7092;96-900-7093;96-900-7094;96-900-7095;96-900-7096;96-900-7097;96-900-7098;96-900-7099;96-900-
 7100;96-900-7101;96-900-7102;96-900-7103;96-900-7104;96-900-7105;96-900-7106;96-900-7107;96-900-
 7108;96-900-7109;96-900-7110;96-900-7111;96-900-7112;96-900-7113;96-900-7114;96-900-7115;96-900-
 7116;96-900-7117;96-900-7118;96-900-7119;96-900-7120;96-900-7121;96-900-7122;96-900-7123;96-900-
 7124;96-900-7125;96-900-7126;96-900-7127;96-900-7128;96-900-7129;96-900-7130;96-900-7131;96-900-
 7132;96-900-7133;96-900-7134;96-900-7135;96-900-7136;96-900-7137;96-900-7181;96-900-7182;96-900-
 7183;96-900-7184;96-900-7185;96-900-7186;96-900-7187;96-900-7188;96-900-7189;96-900-7190;96-900-
 7191;96-900-7192;96-900-7193;96-900-7194;96-900-7195;96-900-7196;96-900-7197;96-900-7198;96-900-
 7199;96-900-7200;96-900-7201;96-900-7202;96-900-7203;96-900-7204;96-900-7205;96-900-7206;96-900-
 7207;96-900-7208;96-900-7209;96-900-7210;96-900-7211;96-900-7212;96-900-7213;96-900-7214;96-900-
 7215;96-900-7216;96-900-7217;96-900-7218;96-900-7219;96-900-7220;96-900-7221;96-900-7222;96-900-
 7223;96-900-7224;96-900-7225;96-900-7226;96-900-7227;96-900-7228;96-900-7229;96-900-7230;96-900-
 7231;96-900-7232;96-900-7233;96-900-7234;96-900-7235;96-900-7236;96-900-7237;96-900-7238;96-900-
 7239;96-900-7240;96-901-0140;96-901-0141;96-901-0142;96-901-0143;96-901-0261;96-901-0343;96-901-
 0344;96-901-0345;96-901-0346;96-901-0347;96-901-0348;96-901-0349;96-901-0350;96-901-0351;96-901-
 0352;96-901-0353;96-901-0354;96-901-0355;96-901-0356;96-901-0357;96-901-0358;96-901-
 3539;96-901-3540;96-901-3541;96-901-3542;96-901-3543;96-901-3544;96-901-3545;96-901-3546;96-901-
 3547;96-901-3548;96-901-3672;96-901-3673;96-901-4109;96-901-4115;96-901-4166;96-901-4227;96-901-
 4255;96-901-4292;96-901-4335;96-901-4387;96-901-4410;96-901-4419;96-901-4431;96-901-4451;96-901-
 4458;96-901-4466;96-901-4500;96-901-4509;96-901-4511;96-901-4527;96-901-4549;96-901-4638;96-901-
 4716;96-901-4718;96-901-4743;96-901-4822;96-901-4829;96-901-4832;96-901-4897;96-901-4924;96-901-
 4960;96-901-4990;96-901-4991;96-901-5021;96-901-5052;96-901-5110;96-901-5180;96-901-5184;96-901-
 5203;96-901-5219;96-901-5257;96-901-5273;96-901-5292;96-901-5305;96-901-5353;96-901-5367;96-901-
 5430;96-901-5450;96-901-5471;96-901-5515;96-901-5540;96-901-5552;96-901-5578;96-901-5590;96-901-
 5627;96-901-5648;96-901-5665;96-901-5706;96-901-5710;96-901-5717;96-901-5760;96-901-5783;96-901-
 5846;96-901-5931;96-901-5947;96-901-5972;96-901-6005;96-901-6008;96-901-6022;96-901-6030;96-901-

6052;96-901-6077;96-901-6091;96-901-6097;96-901-6176;96-901-6239;96-901-6268;96-901-6317;96-901-6329;96-901-6337;96-901-6344;96-901-6363;96-901-6364;96-901-6365;96-901-6371;96-901-6417;96-901-6435;96-901-6475;96-901-6505;96-901-6565;96-901-6578;96-901-6603;96-901-6677;96-901-6699;96-901-6720;96-901-6915;96-901-6916;96-901-6917;96-901-6918;96-901-6919;96-901-7026;96-901-7027;96-901-7028;96-901-7030;96-901-7031;96-901-7032;96-901-7033;96-901-7034;96-901-7035;96-901-7036;96-901-7037;96-901-7038;96-901-7053;96-901-7054;96-901-7055;96-901-7056;96-901-7057;96-201-4618;96-201-4619;96-201-4931;96-220-5377;96-220-7380;96-900-0159;96-900-4189;96-901-0164;96-901-0165;96-901-0166;96-901-0167;96-901-0168;96-901-0169;96-901-0170

Peak List

No.	2theta [°]	d [Å]	I/I0 (peak height)	Counts (peak area)	FWHM	Matched
1	6.45	13.7037	111.48	7.90	0.5333	A
2	10.82	8.1802	56.39	7.03	0.9391	
3	12.45	7.1119	375.61	24.24	0.4858	A,D
4	14.02	6.3182	36.64	1.77	0.3645	C
5	15.45	5.7364	28.60	1.48	0.3885	
6	16.79	5.2805	18.83	1.13	0.4526	
7	18.72	4.7413	408.78	28.96	0.5334	A
8	21.28	4.1757	1000.00	112.47	0.8467	B
9	25.05	3.5551	418.05	23.47	0.4226	A
10	26.64	3.3467	200.90	11.29	0.4230	A,B,C,E
11	31.48	2.8422	79.86	4.35	0.4098	A,C,D
12	33.33	2.6886	311.44	34.83	0.8418	A,B,C,D
13	34.96	2.5664	125.36	21.68	1.3021	A,B,C
14	35.72	2.5136	380.28	33.47	0.6626	B,C,D
15	36.86	2.4389	891.16	89.27	0.7542	A,B,C,E
16	40.35	2.2355	155.06	22.83	1.1082	A,B,C,E
17	41.35	2.1837	148.84	13.41	0.6782	A,B,C,D
18	43.38	2.0860	0.37	0.10	2.0400	A,B,C
19	44.58	2.0326	27.56	3.07	0.8400	A,C
20	45.22	2.0053	42.89	10.64	1.8680	A,B,C
21	47.40	1.9180	33.77	7.99	1.7820	B,C
22	48.52	1.8763	5.83	1.17	1.5076	A,B,C
23	51.00	1.7908	48.48	8.21	1.2757	A,B,C,D,E
24	53.70	1.7069	354.41	62.11	1.3193	A,B,C
25	57.48	1.6033	106.33	9.00	0.6375	A,B,C,E
26	59.24	1.5598	148.97	23.39	1.1821	A,B,C
27	61.76	1.5021	108.12	11.94	0.8315	A,B,C,D
28	63.00	1.4754	105.11	8.32	0.5959	B,C
29	64.18	1.4511	7.58	2.43	2.4131	A,B,C,D,E
30	66.19	1.4120	0.27	0.10	2.7659	A,B,C,D,E
31	66.86	1.3994	42.63	9.64	1.7022	A,C
32	68.80	1.3646	35.38	8.00	1.7022	A,B,C

Integrated Profile Areas

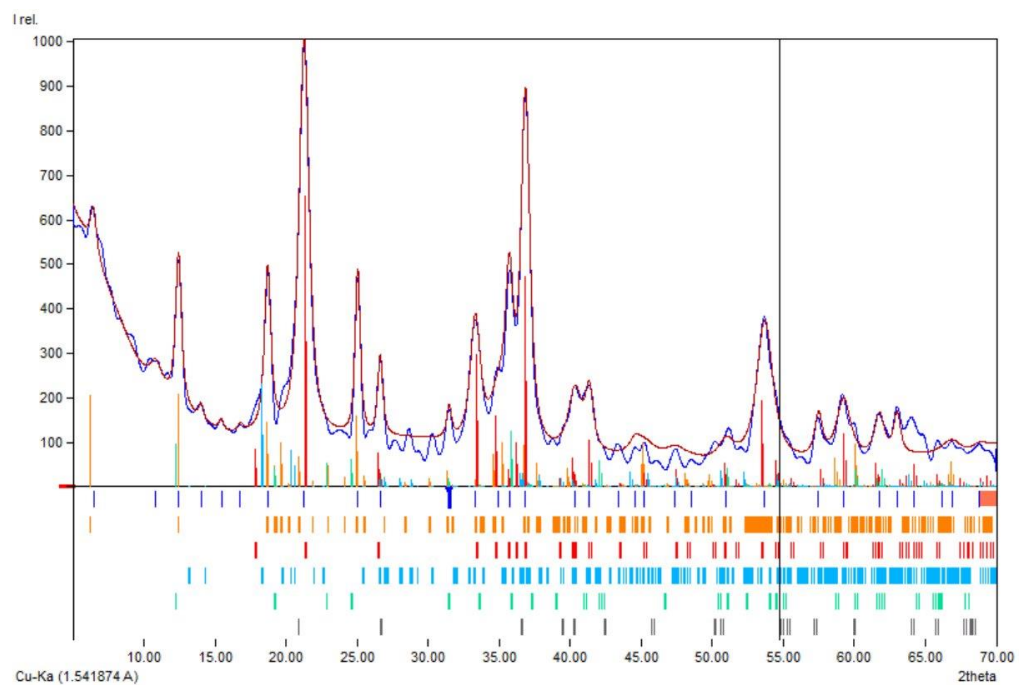
Based on calculated profile

Profile area	Counts	Amount
Overall diffraction profile	73538	100.00%
Background radiation	45253	61.54%
Diffraction peaks	28286	38.46%
Peak area belonging to selected phases	27346	37.19%
Peak area of phase A (Chlorite)	8252	11.22%
Peak area of phase B (Goethite)	13889	18.89%
Peak area of phase C (Gibbsite)	2865	3.90%
Peak area of phase D (Lizardite)	2137	2.91%
Peak area of phase E (Quartz)	203	0.28%
Unidentified peak area	940	1.28%

Peak Residuals

Peak data	Counts	Amount
Overall peak intensity	606	100.00%
Peak intensity belonging to selected phases	504	83.20%
Unidentified peak intensity	102	16.80%

Diffraction Pattern Graphics



Match! Copyright © 2003-2023 CRYSTAL IMPACT, Bonn, Germany

2. Sampel Setelah Pemanggangan Tereduksi dengan Peningkatan Ni Tertinggi pada Suhu Pemanggangan 1000°C dan Fraksi 100 Mesh

Match! Phase Analysis Report

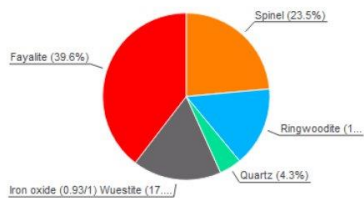
Sample: Shinta-1000C (5-70)

Sample Data

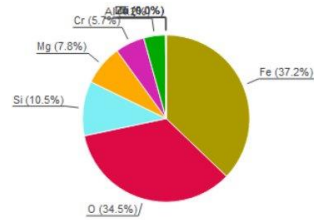
File name	Shinta-1000C.ORG
File path	E:\BISMILLAH TA SHINTA\SKRIPSI\Shinta-1000C
Date collected	Sep 20, 2023 11:57:32
Data range	5.000° - 70.000°
Original data range	5.000° - 70.000°
Number of points	3261
Step size	0.020
Rietveld refinement converged	No
Alpha2 subtracted	No
Background subtr.	No
Data smoothed	Yes
Radiation	X-rays
Wavelength	1.540600 Å

Analysis Results

Phase composition (Weight %)



Elemental composition (Weight %)



Index Amount Name (%)

Index	Amount	Name	Formula sum
A	23.5	Spinel	Al1.129 Cr0.799 Fe0.307 Mg0.736 Mn0.004 Ni0.005 O4 Si0.002 Ti0.005 Zn0.003
B	15.4	Ringwoodite	Mg2 O4 Si
C	4.3	Quartz	O2 Si
D	17.2	Iron oxide (0.93/1) Wuestite	Fe0.932 O
E	39.6	Fayalite	Fe2 O4 Si
6.8		Unidentified peak area	

Amounts calculated by RIR (Reference Intensity Ratio) method

Element Amount (weight %)

Fe	37.2%
O	34.5% (*)
Si	10.5%
Mg	7.8%
Cr	5.7%
Al	4.2%
Ni	0.0%
Ti	0.0%
Mn	0.0%
Zn	0.0%
*LE (sum)	34.5%

Details of identified phases

A: Spinel (23.5 %)*

Formula sum	Al1.129 Cr0.799 Fe0.307 Mg0.736 Mn0.004 Ni0.005 O4 Si0.002 Ti0.005 Zn0.003
Entry number	96-900-5621
Figure-of-Merit (FoM)	0.666389*
Total number of peaks	34
Peaks in range	34
Peaks matched	6
Intensity scale factor	0.55*
Space group	F d -3 m
Crystal system	cubic
Unit cell	a= 8.2129 Å
I/c	2.93
Calc. density	4.126 g/cm³
Reference	Carraro A., "Crystal chemistry of Cr-spinels from a suite of spinel peridotite mantlexenoliths from the Predazzo Area (Dolomites, Northern Italy) Sample: CRSP4", European Journal of Mineralogy 15, 681-688 (2003)

B: Ringwoodite (15.4 %)

Formula sum	Mg2 O4 Si
Entry number	96-900-0270
Figure-of-Merit (FoM)	0.000000
Total number of peaks	34
Peaks in range	34
Peaks matched	4
Intensity scale factor	0.26
Space group	F d -3 m
Crystal system	cubic
Unit cell	a= 8.1200 Å
I/c	2.13
Calc. density	3.491 g/cm³
Reference	Baur W. H., "Computer-simulated crystal structures of observed and hypothetical Mg2SiO4 polymorphs of low and high density normal", American Mineralogist 57, 709-731 (1972)

C: Quartz (4.3 %)

Formula sum	O2 Si
Entry number	96-901-2605
Figure-of-Merit (FoM)	0.000000
Total number of peaks	60
Peaks in range	60
Peaks matched	5

Intensity scale factor 0.09
 Space group P 31 2 1
 Crystal system trigonal (hexagonal axes)
 Unit cell $a = 4.5940 \text{ \AA}$ $c = 5.2000 \text{ \AA}$
 I/Ic 2.68
 Calc. density 3.149 g/cm³
 Reference Hazen R. M., Finger L. W., Hemley R. J., Mao H. K., "High-pressure crystal chemistry and amorphization of alpha-quartz Sample: P = 9.5 GPa", Solid State Communications **72**, 507-511 (1989)

D: Iron oxide (0.93/1)**Wuestite (17.2 %)**

Formula sum Fe0.932 O
 Entry number 96-101-1167
 Figure-of-Merit (FoM) 0.000000
 Total number of peaks 10
 Peaks in range 10
 Peaks matched 2
 Intensity scale factor 0.76
 Space group F m -3 m
 Crystal system cubic
 Unit cell $a = 4.2909 \text{ \AA}$
 I/Ic 5.54
 Meas. density 5.660 g/cm³
 Calc. density 5.721 g/cm³
 Reference Jette E R, Foote F, "An x-ray study of the wuestite (Fe O) solid solutions", Journal of Chemical Physics **1**, 29-36 (1938)

E: Fayalite (39.6 %)*

Formula sum Fe2 O4 Si
 Entry number 96-901-1589
 Figure-of-Merit (FoM) 0.000000
 Total number of peaks 378
 Peaks in range 378
 Peaks matched 30
 Intensity scale factor 0.54 *
 Space group P b n m
 Crystal system orthorhombic
 Unit cell $a = 4.8220 \text{ \AA}$ $b = 10.4880 \text{ \AA}$ $c = 6.0940 \text{ \AA}$
 I/Ic 1.70
 Calc. density 4.392 g/cm³
 Reference Kudo Y., Takeda H., "Single crystal X-ray diffraction study on the bond compressibility of fayalite, Fe~2~SiO~4~ and rutile, TiO~2~ under high pressure Sample: P = 0.001 kbar", Physica B+C **140**, 333-336 (1986)

(*2theta values have been shifted internally for the calculation of the amounts, the intensity scaling factors as well as the figure-of-merit (FoM), due to the active search-match option 'Automatic zero point adaption'.

Candidates

Name	Formula	Entry No.	FoM
	Fe2 Si	96-901-4529	0.7055
	Fe Sb	96-900-8895	0.7030
Dolomite	C Ca0.5 Mg0.5 O3	96-900-3521	0.6855
Sr3 Sn2 O7	O7 Sn2 Sr3	96-152-1095	0.6829
Dolomite	C Ca0.5 Mg0.5 O3	96-900-3520	0.6819
Dolomite	C Ca0.5 Mg0.5 O3	96-900-3522	0.6800
Zr50 Sc12 O118	O118 Sc12 Zr50	96-153-6706	0.6763
SrSiO3 (SrSiO3 cubic perovskite at 37.8 GPa)	O3 Si Sr	96-155-7931	0.6735
Dolomite	C2 Ca1.14 Mg0.86 O6	96-900-4934	0.6730
Dolomite	C2 Ca Mg O6	96-900-0084	0.6711
	Ni Sn	96-900-8906	0.6669
Dolomite	C2 Ca Mg O6	96-900-1007	0.6665
Dolomite	C2 Ca Mg O6	96-900-1011	0.6665
Ba2 Nb (Nb2.5 V1.5) O9	Ba2 Nb3.5 O9 V1.5	96-153-1604	0.6661
Ag3.5 Si	Ag3.5 I S	96-150-9831	0.6647
Dolomite	C2 Ca Fe0.33 Mg0.67 O6	96-900-4935	0.6641
Dolomite	C2 Ca1.13 Mg0.87 O6	96-900-4932	0.6631
Ankerite	C2 Ca1.007 Fe0.542 Mg0.451 O6	96-900-1247	0.6616
Dolomite	C2 Ca Mg O6	96-900-0106	0.6600
Dolomite	C Ca0.5 Mg0.5 O3	96-900-0888	0.6589
Dolomite	C Ca0.5 Mg0.5 O3	96-900-3524	0.6568
Magnesium Calcium Carbonate (.1/.9/1) (Dolomite)	C2 Ca Mg O6	96-151-7797	0.6555
Calcium magnesium cobalt dicarbonate	C2 Ca Co0.17 Mg0.83 O6	96-224-0440	0.6551
Calcium Magnesium Carbonate (Dolomite)	C2 Ca Mg O6	96-210-5964	0.6539
Dolomite	C2 Ca1.07 Mg0.93 O6	96-900-4933	0.6536
Dolomite	C2 Ca Mg O6	96-900-1006	0.6528
Dolomite	C2 Ca Mg O6	96-900-1010	0.6528
	U	96-153-9737	0.6527
lead hafnate titanate	Hf0.8 O3 Pb Ti0.2	96-210-2004	0.6521
Dolomite	C2 Ca1.08 Mg0.92 O6	96-900-4929	0.6519
Dolomite	C2 Ca Fe0.05 Mg0.94 Mn0.01 O6	96-901-7357	0.6517
Dolomite	C2 Ca1.07 Mg0.93 O6	96-900-4931	0.6512
Calcium magnesium carbonate (Dolomite)	C2 Ca Mg O6	96-120-0015	0.6510
Calcium magnesium carbonate (Dolomite)	C2 Ca Mg O6	96-500-0117	0.6510
Dolomite	C2 Ca Fe0.05 Mg0.94 Mn0.01 O6	96-900-9593	0.6510
Dolomite	C2 Ca Mg O6	96-900-1044	0.6499
Dolomite	C Ca0.5 Mg0.5 O3	96-900-3526	0.6497
Dolomite	C2 Ca0.997 Fe0.234 Mg0.769 O6	96-900-1246	0.6469
	Ba Col1.4 Fe0.4 O2.426 Zr0.2	96-156-7215	0.6434
Silver selenide - S-alpha	Ag2 Se	96-101-1339	0.6430
Cu15 (B2 O5)2 (B O3)6 O2	B10 Cu15 O30	96-210-5419	0.6423
Ba (Sn O3)	Ba O3 Sn	96-153-8371	0.6415
barium tantalum oxynitride	Au Rb	96-151-0281	0.6397
(Ga Pu)	Ba N0.76 O2.24 Ta	96-49-9034	0.6393
barium tantalum oxynitride	Fe2 O7 P2	96-40-0292	0.6384
Ankerite	Ga Pu	96-152-3831	0.6375
Silver niobium sulfide (0.6/1/2)	Ba N0.58 O2.42 Ta	96-451-9033	0.6372
Lead Barium Zirconium Titanium Oxide	Li P	96-152-3815	0.6337
	C2 Ca0.997 Fe0.676 Mg0.273 Mn0.054 O695-900-1413	96-6360	
	Ag0.6 Nb S2	96-150-9008	0.6348
	Ba0.3 O3 Pb0.7 Ti0.35 Zr0.65	96-210-2952	0.6342
	Ba Li0.2 N0.19 O2.81 Ta0.8	96-451-2486	0.6339

and 1064 others...

Search-Match**Settings**

Reference database used COD-Inorg 2023.06.06
 Automatic zeropoint adaptation Yes

Downgrade entries with low scaling factors	Yes
Minimum figure-of-merit (FOM)	0.60
2theta window for peak corr.	0.30 deg
Minimum rel. int. for peak corr.	0
Parameter/influence 2theta	0.50
Parameter/influence intensities	0.50
Parameter multiple/single phase(s)	0.50

Criteria for entries added by user

References

Entry number:

Peak List

No.	θ [θ]	d [Å]	I/I₀ (peak height)	Counts (peak area)	FWHM	Matched
1	25.12	3.5429	379.05	21.95	0.3684	E
2	29.40	3.0356	60.72	8.08	0.8468	E
3	30.86	2.8952	435.58	49.81	0.7275	A
4	31.08	2.8752	117.55	8.13	0.4400	B

5	31.66	2.8238	536.21	19.98	0.2370	E
6	34.10	2.6272	173.12	10.47	0.3847	E
7	35.04	2.5588	390.79	26.37	0.4294	E
8	35.98	2.4941	1000.00	102.31	0.6509	E
9	36.44	2.4636	689.28	38.41	0.3545	A,B,D
10	37.38	2.4038	141.31	9.77	0.4400	E
11	39.14	2.2997	127.13	15.78	0.7898	C,E
12	41.27	2.1859	67.45	4.39	0.4138	C,E
13	43.80	2.0652	783.48	33.88	0.2751	A,E
14	44.60	2.0299	323.08	32.25	0.6350	B
15	49.55	1.8380	74.28	5.08	0.4354	E
16	51.02	1.7886	208.29	8.37	0.2558	
17	52.00	1.7573	72.07	6.97	0.6150	E
18	54.76	1.6750	98.96	22.05	1.4174	A,E
19	58.28	1.5820	156.17	21.56	0.8783	A,C,E
20	58.80	1.5693	157.65	10.18	0.4109	B
21	61.02	1.5173	115.73	13.79	0.7579	D,E
22	64.23	1.4490	208.48	43.29	1.3211	A,E
23	64.54	1.4428	133.52	3.82	0.1822	C,E

Integrated Profile Areas

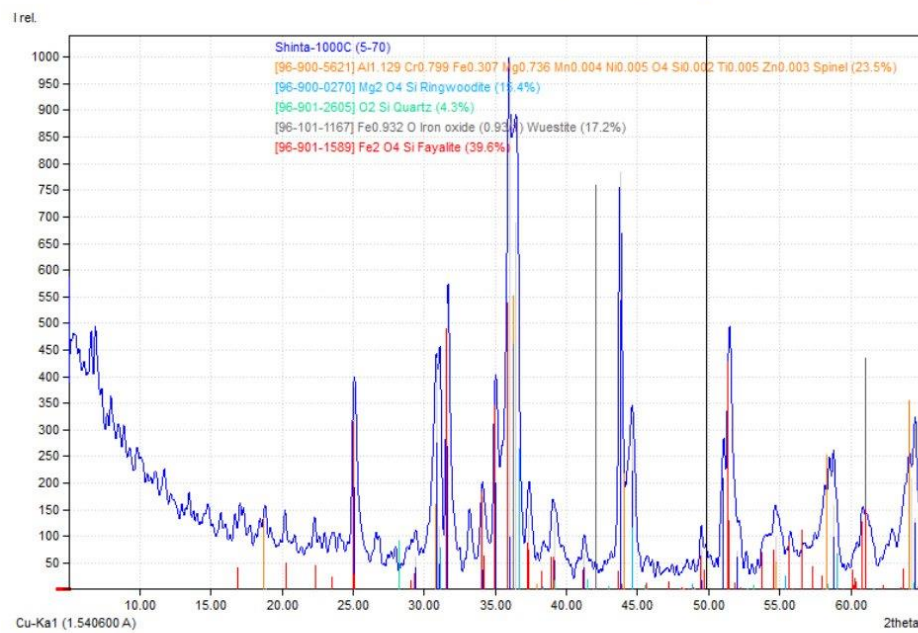
Based on calculated profile

Profile area	Counts	Amount
Overall diffraction profile	62715	100.00%
Background radiation	35808	57.10%
Diffraction peaks	26907	42.90%
Peak area belonging to selected phases	22644	36.11%
Peak area of phase A (Spinel)	5833	9.30%
Peak area of phase B (Ringwoodite)	2362	3.77%
Peak area of phase C (Quartz)	406	0.65%
Peak area of phase D (Iron oxide (0.93/1) Wuestite)	2173	3.47%
Peak area of phase E (Fayalite)	11869	18.93%
Unidentified peak area	4263	6.80%

Peak Residuals

Peak data	Counts	Amount
Overall peak intensity	517	100.00%
Peak intensity belonging to selected phases	368	71.16%
Unidentified peak intensity	149	28.84%

Diffraction Pattern Graphics



LAMPIRAN 2

HASIL ANALISIS X-RAY FLUORESCENCE (XRF)

HASIL ANALISIS XRF

Sample id	Kadar Unsur/ Senyawaan yang dianalisa sesuai dengan komoditi (%)														
Element Dimension	Ni	Co	Fe	Cr	Na ₂ O	MgO	Al ₂ O ₃	SiO ₂	K ₂ O	CaO	TiO ₂	Cr ₂ O ₃	MnO	Fe ₂ O ₃	
Detection Limit	0,005	0,001	0,01	0,005	0,01	0,01	0,01	0,01	0,001	0,003	0,01	0,005	0,01	0,01	0,01
Method	WDXRF	WDXRF	WDXRF	WDXRF	WDXRF	WDXRF	WDXRF	WDXRF	WDXRF	WDXRF	WDXRF	WDXRF	WDXRF	WDXRF	WDXRF
Unit	%	%	%	%	%	%	%	%	%	%	%	%	%	%	%
DS 001 ORI	1,52	0,03	37,47	2,03	0,01	2,63	10,69	12,16	0,00	0,06	0,23	2,97	0,45	53,59	
DS 002 ORI	1,60	0,05	39,82	2,17	0,03	3,27	12,67	14,72	0,29	0,06	0,24	3,17	0,63	56,95	
DS 003 ORI	1,51	0,04	40,17	2,13	0,02	2,99	12,92	13,79	0,29	0,09	0,24	3,11	0,59	57,45	
DS 004 ORI	1,41	0,05	38,97	1,94	0,02	2,92	12,75	13,45	0,27	0,08	0,24	2,84	0,63	55,72	
DS 005 ORI	1,63	0,05	41,19	2,24	0,01	3,63	13,48	15,42	0,29	0,07	0,25	3,27	0,71	58,90	
DS 006 ORI	1,52	0,04	41,20	2,11	0,03	3,04	12,81	13,85	0,28	0,08	0,25	3,09	0,60	58,91	
DS 007 ORI	1,51	0,05	40,97	2,11	0,03	3,13	13,55	14,24	0,28	0,07	0,26	3,08	0,61	58,59	
DS 008 ORI	1,74	0,06	42,87	2,40	0,02	3,83	14,42	16,48	0,26	0,06	0,27	3,51	0,75	61,31	
DS 009 ORI	1,71	0,05	43,58	2,36	0,05	3,50	14,43	15,59	0,22	0,07	0,27	3,45	0,63	62,31	
DS 010 ORI	1,64	0,04	46,08	2,39	0,06	3,65	14,56	15,69	0,19	0,08	0,29	3,50	0,62	65,89	
DS 011 ORI	1,63	0,09	44,95	2,49	0,08	4,91	16,56	16,34	0,24	0,06	0,29	3,64	1,30	64,28	
DS 012 ORI	1,73	0,04	47,98	2,53	0,05	4,01	15,39	16,50	0,26	0,07	0,29	3,70	0,67	68,62	
DS 013 ORI	1,66	0,04	47,01	2,46	0,12	3,78	14,99	15,87	0,27	0,08	0,30	3,60	0,60	67,22	

LAMPIRAN 3
PERHITUNGAN *RECOVERY*

A. Nikel

Suhu (°C)	Ukuran fraksi (Mesh)	Kadar awal Ni (%)	Berat sampel awal + reduktor (gr)	Berat setelah roasting (gr)	Kadar akhir Ni (%)	Recovery Ni (%)
800	100	1,52	20	16,1	1,60	84,58
	150	1,52	20	16,0	1,51	79,41
	200	1,52	20	16,1	1,41	74,47
900	100	1,52	20	15,4	1,63	82,58
	150	1,52	20	15,2	1,52	76,25
	200	1,52	20	15,5	1,51	76,89
1000	100	1,52	20	14,6	1,74	83,36
	150	1,52	20	14,5	1,71	81,76
	200	1,52	20	14,4	1,64	77,60
1100	100	1,52	20	13,5	1,63	72,35
	150	1,52	20	13,6	1,73	77,23
	200	1,52	20	13,3	1,66	72,36

Recovery Ni dihitung menggunakan rumus sebagai berikut:

$$\text{Recovery (\%)} = \frac{\text{Berat sampel setelah pemanggangan} \times \text{kadar akhir Ni}}{\text{Berat sampel awal} \times \text{kadar awal Ni}} \times 100\%$$

1. Recovery Ni pada suhu 800°C menggunakan fraksi 100 mesh

$$\text{Recovery (\%)} = \frac{\text{Berat sampel setelah pemanggangan} \times \text{kadar akhir Ni}}{\text{Berat sampel awal} \times \text{kadar awal Ni}} \times 100\%$$

$$\text{Recovery (\%)} = \frac{16,1 \text{ (gr)} \times 1,60 \text{ (\%)}}{20 \text{ (gr)} \times 1,52 \text{ (\%)}} \times 100\%$$

$$\text{Recovery (\%)} = 84,58\%$$

2. Recovery Ni pada suhu 800°C menggunakan fraksi 150 mesh

$$\text{Recovery (\%)} = \frac{\text{Berat sampel setelah pemanggangan} \times \text{kadar akhir Ni}}{\text{Berat sampel awal} \times \text{kadar awal Ni}} \times 100\%$$

$$\text{Recovery (\%)} = \frac{16 \text{ (gr)} \times 1,51 \text{ (\%)}}{20 \text{ (gr)} \times 1,52 \text{ (\%)}} \times 100\%$$

$$\text{Recovery (\%)} = 79,41\%$$

3. Recovery Ni pada suhu 800°C menggunakan fraksi 200 mesh

$$\text{Recovery (\%)} = \frac{\text{Berat sampel setelah pemanggangan} \times \text{kadar akhir Ni}}{\text{Berat sampel awal} \times \text{kadar awal Ni}} \times 100\%$$

$$\text{Recovery (\%)} = \frac{16,1 \text{ (gr)} \times 1,41 \text{ (\%)}}{20 \text{ (gr)} \times 1,52 \text{ (\%)}} \times 100\%$$

$$\text{Recovery (\%)} = 74,47\%$$

4. Recovery Ni pada suhu 900°C menggunakan fraksi 100 mesh

$$\text{Recovery (\%)} = \frac{\text{Berat sampel setelah pemanggangan} \times \text{kadar akhir Ni}}{\text{Berat sampel awal} \times \text{kadar awal Ni}} \times 100\%$$

$$\text{Recovery (\%)} = \frac{15,4 \text{ (gr)} \times 1,63 \text{ (\%)}}{20 \text{ (gr)} \times 1,52 \text{ (\%)}} \times 100\%$$

$$\text{Recovery (\%)} = 82,58\%$$

5. Recovery Ni pada suhu 900°C menggunakan fraksi 150 mesh

$$\text{Recovery (\%)} = \frac{\text{Berat sampel setelah pemanggangan} \times \text{kadar akhir Ni}}{\text{Berat sampel awal} \times \text{kadar awal Ni}} \times 100\%$$

$$\text{Recovery (\%)} = \frac{15,2 \text{ (gr)} \times 1,52 \text{ (\%)}}{20 \text{ (gr)} \times 1,52 \text{ (\%)}} \times 100\%$$

$$\text{Recovery (\%)} = 76,25\%$$

6. Recovery Ni pada suhu 900°C menggunakan fraksi 200 mesh

$$\text{Recovery (\%)} = \frac{\text{Berat sampel setelah pemanggangan} \times \text{kadar akhir Ni}}{\text{Berat sampel awal} \times \text{kadar awal Ni}} \times 100\%$$

$$\text{Recovery (\%)} = \frac{15,5 \text{ (gr)} \times 1,51 \text{ (\%)}}{20 \text{ (gr)} \times 1,52 \text{ (\%)}} \times 100\%$$

$$\text{Recovery (\%)} = 76,89\%$$

7. Recovery Ni pada suhu 1000°C menggunakan fraksi 100 mesh

$$\text{Recovery (\%)} = \frac{\text{Berat sampel setelah pemanggangan} \times \text{kadar akhir Ni}}{\text{Berat sampel awal} \times \text{kadar awal Ni}} \times 100\%$$

$$\text{Recovery (\%)} = \frac{14,6 \text{ (gr)} \times 1,74 \text{ (\%)}}{20 \text{ (gr)} \times 1,52 \text{ (\%)}} \times 100\%$$

$$\text{Recovery (\%)} = 83,36\%$$

8. Recovery Ni pada suhu 1000°C menggunakan fraksi 150 mesh

$$\text{Recovery (\%)} = \frac{\text{Berat sampel setelah pemanggangan} \times \text{kadar akhir Ni}}{\text{Berat sampel awal} \times \text{kadar awal Ni}} \times 100\%$$

$$\text{Recovery (\%)} = \frac{14,5 \text{ (gr)} \times 1,71 \text{ (\%)}}{20 \text{ (gr)} \times 1,52 \text{ (\%)}} \times 100\%$$

$$\text{Recovery (\%)} = 81,76\%$$

9. Recovery Ni pada suhu 1000°C menggunakan fraksi 200 mesh

$$\text{Recovery (\%)} = \frac{\text{Berat sampel setelah pemanggangan} \times \text{kadar akhir Ni}}{\text{Berat sampel awal} \times \text{kadar awal Ni}} \times 100\%$$

$$\text{Recovery (\%)} = \frac{14,4 \text{ (gr)} \times 1,64 \text{ (\%)}}{20 \text{ (gr)} \times 1,52 \text{ (\%)}} \times 100\%$$

$$\text{Recovery (\%)} = 77,60\%$$

10. Recovery Ni pada suhu 1100°C menggunakan fraksi 100 mesh

$$Recovery (\%) = \frac{Berat sampel setelah pemanggangan x kadar akhir Ni}{Berat sampel awal x kadar awal Ni} \times 100\%$$

$$Recovery (\%) = \frac{13,5 (gr) x 1,63 (\%)}{20 (gr) x 1,52 (\%)} \times 100\%$$

$$Recovery (\%) = 72,35\%$$

11. Recovery Ni pada suhu 1100°C menggunakan fraksi 150 mesh

$$Recovery (\%) = \frac{Berat sampel setelah pemanggangan x kadar akhir Ni}{Berat sampel awal x kadar awal Ni} \times 100\%$$

$$Recovery (\%) = \frac{13,6 (gr) x 1,63 (\%)}{20 (gr) x 1,52 (\%)} \times 100\%$$

$$Recovery (\%) = 77,23\%$$

12. Recovery Ni pada suhu 1100°C menggunakan fraksi 150 mesh

$$Recovery (\%) = \frac{Berat sampel setelah pemanggangan x kadar akhir Ni}{Berat sampel awal x kadar awal Ni} \times 100\%$$

$$Recovery (\%) = \frac{13,3 (gr) x 1,66 (\%)}{20 (gr) x 1,52 (\%)} \times 100\%$$

$$Recovery (\%) = 72,36\%$$

B. Iron

Suhu (°C)	Ukuran fraksi (Mesh)	Kadar awal Fe (%)	Berat awal sampel + reduktor (gr)	Berat sampel akhir (gr)	Kadar akhir Fe (%)	Recovery Fe (%)
800	100	37,47	20	16,1	39,82	85,40
	150	37,47	20	16,0	40,17	85,70
	200	37,47	20	16,1	38,97	83,49
900	100	37,47	20	15,4	41,19	84,65
	150	37,47	20	15,2	41,20	83,84
	200	37,47	20	15,5	40,97	84,63
1000	100	37,47	20	14,6	42,87	83,31
	150	37,47	20	14,5	43,58	84,53
	200	37,47	20	14,4	46,08	88,45
1100	100	37,47	20	13,5	44,95	80,94
	150	37,47	20	13,6	47,98	86,89
	200	37,47	20	13,3	47,01	83,12

Recovery Fe dihitung menggunakan rumus sebagai berikut:

$$Recovery (\%) = \frac{Berat sampel setelah pemanggangan x kadar akhir Fe}{Berat sampel awal x kadar awal Fe} \times 100\%$$

1. Recovery Fe pada suhu 800°C menggunakan fraksi 100 mesh

$$\text{Recovery (\%)} = \frac{\text{Berat sampel setelah pemanggangan} \times \text{kadar akhir Fe}}{\text{Berat sampel awal} \times \text{kadar awal Fe}} \times 100\%$$

$$\text{Recovery (\%)} = \frac{16,1 \text{ (gr)} \times 39,82 \%}{20 \text{ (gr)} \times 37,47 \%} \times 100\%$$

$$\text{Recovery (\%)} = 85,40\%$$

2. Recovery Fe pada suhu 800°C menggunakan fraksi 150 mesh

$$\text{Recovery (\%)} = \frac{\text{Berat sampel setelah pemanggangan} \times \text{kadar akhir Fe}}{\text{Berat sampel awal} \times \text{kadar awal Fe}} \times 100\%$$

$$\text{Recovery (\%)} = \frac{16 \text{ (gr)} \times 40,17 \%}{20 \text{ (gr)} \times 37,47 \%} \times 100\%$$

$$\text{Recovery (\%)} = 85,70\%$$

3. Recovery Fe pada suhu 800°C menggunakan fraksi 200 mesh

$$\text{Recovery (\%)} = \frac{\text{Berat sampel setelah pemanggangan} \times \text{kadar akhir Fe}}{\text{Berat sampel awal} \times \text{kadar awal Fe}} \times 100\%$$

$$\text{Recovery (\%)} = \frac{16,1 \text{ (gr)} \times 38,97 \%}{20 \text{ (gr)} \times 37,47 \%} \times 100\%$$

$$\text{Recovery (\%)} = 83,49\%$$

4. Recovery Fe pada suhu 900°C menggunakan fraksi 100 mesh

$$\text{Recovery (\%)} = \frac{\text{Berat sampel setelah pemanggangan} \times \text{kadar akhir Fe}}{\text{Berat sampel awal} \times \text{kadar awal Fe}} \times 100\%$$

$$\text{Recovery (\%)} = \frac{15,4 \text{ (gr)} \times 41,19 \%}{20 \text{ (gr)} \times 37,47 \%} \times 100\%$$

$$\text{Recovery (\%)} = 84,65\%$$

5. Recovery Fe pada suhu 900°C menggunakan fraksi 150 mesh

$$\text{Recovery (\%)} = \frac{\text{Berat sampel setelah pemanggangan} \times \text{kadar akhir Fe}}{\text{Berat sampel awal} \times \text{kadar awal Fe}} \times 100\%$$

$$\text{Recovery (\%)} = \frac{15,2 \text{ (gr)} \times 41,20 \%}{20 \text{ (gr)} \times 37,47 \%} \times 100\%$$

$$\text{Recovery (\%)} = 83,84\%$$

6. Recovery Fe pada suhu 900°C menggunakan fraksi 200 mesh

$$\text{Recovery (\%)} = \frac{\text{Berat sampel setelah pemanggangan} \times \text{kadar akhir Fe}}{\text{Berat sampel awal} \times \text{kadar awal Fe}} \times 100\%$$

$$\text{Recovery (\%)} = \frac{15,5 \text{ (gr)} \times 40,97 \%}{20 \text{ (gr)} \times 37,47 \%} \times 100\%$$

$$\text{Recovery (\%)} = 83,63\%$$

7. Recovery Fe pada suhu 1000°C menggunakan fraksi 100 mesh

$$\text{Recovery (\%)} = \frac{\text{Berat sampel setelah pemanggangan} \times \text{kadar akhir Fe}}{\text{Berat sampel awal} \times \text{kadar awal Fe}} \times 100\%$$

$$\text{Recovery (\%)} = \frac{14,6 \text{ (gr)} \times 42,87 \%}{20 \text{ (gr)} \times 37,47 \%} \times 100\%$$

$$\text{Recovery (\%)} = 83,31\%$$

8. Recovery Fe pada suhu 1000°C menggunakan fraksi 150 mesh

$$\text{Recovery (\%)} = \frac{\text{Berat sampel setelah pemanggangan} \times \text{kadar akhir Fe}}{\text{Berat sampel awal} \times \text{kadar awal Fe}} \times 100\%$$

$$\text{Recovery (\%)} = \frac{14,5 \text{ (gr)} \times 43,58 \%}{20 \text{ (gr)} \times 37,47 \%} \times 100\%$$

$$\text{Recovery (\%)} = 84,53\%$$

9. Recovery Fe pada suhu 1000°C menggunakan fraksi 200 mesh

$$\text{Recovery (\%)} = \frac{\text{Berat sampel setelah pemanggangan} \times \text{kadar akhir Fe}}{\text{Berat sampel awal} \times \text{kadar awal Fe}} \times 100\%$$

$$\text{Recovery (\%)} = \frac{14,4 \text{ (gr)} \times 46,08 \%}{20 \text{ (gr)} \times 37,47 \%} \times 100\%$$

$$\text{Recovery (\%)} = 88,45\%$$

10. Recovery Fe pada suhu 1100°C menggunakan fraksi 100 mesh

$$\text{Recovery (\%)} = \frac{\text{Berat sampel setelah pemanggangan} \times \text{kadar akhir Fe}}{\text{Berat sampel awal} \times \text{kadar awal Fe}} \times 100\%$$

$$\text{Recovery (\%)} = \frac{13,5 \text{ (gr)} \times 44,95 \%}{20 \text{ (gr)} \times 37,47 \%} \times 100\%$$

$$\text{Recovery (\%)} = 80,94\%$$

11. Recovery Fe pada suhu 1100°C menggunakan fraksi 150 mesh

$$\text{Recovery (\%)} = \frac{\text{Berat sampel setelah pemanggangan} \times \text{kadar akhir Fe}}{\text{Berat sampel awal} \times \text{kadar awal Fe}} \times 100\%$$

$$\text{Recovery (\%)} = \frac{13,6 \text{ (gr)} \times 47,98 \%}{20 \text{ (gr)} \times 37,47 \%} \times 100\%$$

$$\text{Recovery (\%)} = 86,89\%$$

12. Recovery Fe pada suhu 1100°C menggunakan fraksi 200 mesh

$$\text{Recovery (\%)} = \frac{\text{Berat sampel setelah pemanggangan} \times \text{kadar akhir Fe}}{\text{Berat sampel awal} \times \text{kadar awal Fe}} \times 100\%$$

$$\text{Recovery (\%)} = \frac{13,3 \text{ (gr)} \times 47,01 \%}{20 \text{ (gr)} \times 37,47 \%} \times 100\%$$

$$\text{Recovery (\%)} = 83,12\%$$